

MOL 35543

TITLE PAGE.

**MOLECULAR INTERACTION OF A POTENT NON-PEPTIDE AGONIST
WITH THE CHEMOKINE RECEPTOR CCR8**

Pia C. Jensen, Rie Nygaard, Stefanie Thiele, Amy Elder, Guoming Zhu, Roland Kolbeck,
Shomir Ghosh, Thue W Schwartz, and Mette M. Rosenkilde*

¹Lab. for Molecular Pharmacology, Dep. of Pharmacology, Copenhagen University, Denmark (PCJ, RN,
ST, TWS, MMR)

²Millennium Pharmaceuticals, MIT, Cambridge, Boston, MA, US (AE, GZ, RK, SG)

MOL 35543

RUNNING TITE PAGE.

a) Running title: Non-peptide agonist and antagonists interact with GluVII:06.

b) Address correspondence to:

Mette M. Rosenkilde, Laboratory for Molecular Pharmacology,

Department of Pharmacology, The Panum Institute, Copenhagen University,

Blegdamsvej 2, 2200 Copenhagen, Denmark,

Phone: 0045 61364871, Fax : 0045 35327610, e-mail: rosenkilde@molpharm.dk

c) Numbering:

Number of text pages: 33

Number of tables: 2

Number of figures: 10

Number of references: 40

Number of words in the abstract: 252

Number of words in the introduction: 665

Number of words in the discussion: 1499

d) Nonstandard abbreviations: 7TM receptors (7 transmembrane spanning α -helixreceptors), Th2 cells (T-helper 2 cells), CCL (CC-chemokine), CXCL (CXC-chemokine), IP (inositole phosphates), LMD-009 (8-[3-(2-methoxyphenoxy)benzyl]-1-phenethyl-1,3,8-triaza-spiro[4.5]decan-4-one), LMD-584 (2-(1-(3-(2-methoxyphenoxy)benzyl)-4-hydroxypiperidin-4-yl)benzoic acid), LMD-902 (N-ethyl-2-4-methoxybenzenesulfonamide), LMD-268 (N-(1-(3-(2-methoxyphenoxy)benzyl)piperidin-4-yl)-2-phenyl-4-(pyrrolidin-1-yl)butanamide), LMD-174 (N-(1-(3-(2-methoxyphenoxy)benzyl)piperidin-4-yl)-1,2,3,4-tetrahydro-2-oxoquinoline-4-carboxamide), ZK 756326 (2-[2-[4-(3-Phenoxybenzyl)piperazin-1-yl]ethoxy]ethanol), BX471 (R-N-[5-chloro-2-[2-[4-[(4-fluorophenyl)methyl]-2-methyl-1-piperazinyl]-2-oxoethoxy]phenyl]urea), ELISA (Surface Enzyme-Linked Immunosorbent Assay).

MOL 35543

Abstract

Most non-peptide *antagonists* for CC-chemokine receptors share a common pharmacophore with a centrally located, positively charged amine that interacts with the highly conserved glutamic acid (Glu) located in position 6 of transmembrane helix VII (VII:06). We present a novel CCR8 non-peptide *agonist*, LMD-009 that also contains a centrally located, positively charged amine. LMD-009 selectively stimulated CCR8 among the 20 identified human chemokine receptors. It mediated chemotaxis, inositol-phosphate accumulation and calcium release with high potencies (EC_{50} from 11 to 87 nM) and with efficacies similar to the endogenous agonist CCL1, and competed for ^{125}I -CCL1 binding with an affinity of 66 nM. A series of 29 mutations targeting 25 amino acids broadly distributed in the minor and major ligand-binding pockets of CCR8 uncovered that the binding of LMD-009 and of four analogs (LMD584, -902, -268, and -174) included several key-residues for non-peptide antagonists targeting CCR1, -2 and -5. Importantly, a nearly 1000-fold decrease in potency was observed for all five compounds for the Ala substitution of the anchor-point GluVII:06 (Glu²⁸⁶) and a 19-fold gain-of-function was observed for LMD-009 (but not the four other analogs) for the Ala substitution of PheVI:16 (Phe²⁵⁴). These structural hallmarks were particularly important in the generation of a model of the molecular mechanism of action for LMD-009. In conclusion, we present the first molecular mapping of the interaction of a *non-peptide agonist* with a chemokine receptor, and show that the binding pocket of LMD-009 and of analogs overlaps considerably with the binding pockets of CC-chemokine receptor *non-peptide antagonists* in general.

MOL 35543

Introduction

Chemokine receptors belong to the superfamily of rhodopsin-like G protein-coupled 7TM receptors (Murphy et al., 2000). The chemokine ligands (chemotactic cytokines) are a family of large peptides (70-80 amino acids in length) composed of around 50 members. The CC-chemokines are characterized by the absence of an amino acid between the first two of four conserved cysteines and constitute the largest group (CCL1-28), whereas the CXC-chemokines constitute the other major group (CXCL1-16). Two additional chemokines, the XCL1 and the CX3CL1 have been described (Murphy et al., 2000). The chemokine system regulates the development, activation and recruitment of leukocytes, and also exerts important roles outside the immune system, for instance on organogenesis, angiogenesis and carcinogenesis (Gerard and Rollins, 2001). CCR8 is selectively expressed on a subset of T-helper-2 (Th2) and regulatory T-cells and is upregulated on Th2 cells upon activation (Soler et al., 2006). Activated Th2 cells produce the cytokines IL-4, IL-5 and IL-13, which are important mediators of inflammation and airway hyperreactivity in bronchial asthma, and CCR8 deficiency has been shown to ameliorate lung inflammation and airway function in the mouse (Chensue et al., 2001). CCR8 also seems to play an important role in CNS pathology as it is expressed on phagocytic macrophages and activated microglial cells in the CNS, in active demyelinating multiple sclerosis (MS), progressive multifocal leukoencephalopathy (PML) and in cerebral ischemic lesions (Trebst et al., 2003).

In contrast to many other CC and CXC-chemokine receptors, that are rather promiscuous in their ligand-binding profile, CCR8 only binds one endogenous chemokine CCL1 (I-309) and CCL1 only interacts with this one receptor. There are only a few additional chemokine/receptor pairs with a similar stringency, for example CXCL12 (SDF-1)/CXCR4 and CX3CL1 (fractalkine)/CX3CR1 (Murphy et al., 2000). However, additional virus-encoded CC-chemokines targeting CCR8 have been described, indicating a potential role for CCR8 in infectious diseases. For example the CCR8 antagonist, MC148, encoded by the poxvirus

MOL 35543

Molluscum contagiosum (Damon et al., 1998) and the two CCR8 agonists, vCCL1 and vCCL2 encoded by human herpesvirus 8 (Dairaghi et al., 1999).

Many pharmaceutical companies wish to develop chemokine receptor non-peptide antagonists due to the well documented functions of the chemokine system in immune system surveillance and pathological inflammatory processes. Presently, the research in chemokine non-peptide antagonists has resulted in ~250 patent applications and nine clinical trials (Wells et al., 2006; Horuk, 2003). Indeed, non-peptide antagonists have today been identified for the majority of chemokine receptors. However, CCR8 differs from these since agonists, instead of antagonists, appear from screening efforts (ie. CCR8 is agonist-prone). Thus, a micromolar non-peptide agonist, ZK 756326 (2-[2-[4-(3-Phenoxybenzyl)piperazin-1-yl]ethoxy]ethanol), has recently been described for CCR8 (Haskell et al., 2006), and vCCL2 (that in general acts like a broad-spectrum chemokine antagonist) also activates this receptor (Dairaghi et al., 1999). We present here a novel high-affinity non-peptide agonist for CCR8, LMD-009, that acts in the nanomolar range with the same efficacy and potency as CCL1. The structure of LMD-009 has some similarities to ZK 756326 (Haskell et al., 2006). Both compounds contain a central amine - as observed for many chemokine receptor non-peptide antagonists (Rosenkilde and Schwartz, 2006) - and an aromatic group (biphenyl) on the “right side”, with the only difference being an ortho-methoxy group in the terminal phenyl of LMD-009. The central amine source differs slightly, since LMD-009 contains a spiro-ring system with a piperidine, whereas the ZK 756326 contains a piperazine. The greatest difference is found on the “left side”, as LMD-009 contains an aromatic group (phenethylimidazoline-4-one) that in ZK 756326 is an ethoxyethanol (Fig. 1). Mutational mapping of LMD-009 and a series of analogs of this in a library of 27 mutants covering the main ligand-binding pocket of CCR8 demonstrated that the highly

MOL 35543

conserved Glu at position 6 in the extracellular end of TM-VII (VII:06¹) (Rosenkilde and Schwartz, 2006) is essential for the action of LMD-009. Additionally, we find that aromatic residues in the binding pocket, which are believed to interact with the non-peptide antagonists in other chemokine receptors, also are important for the binding of LMD-009.

¹ In the text we use the generic 7TM numbering system suggested by Baldwin (Baldwin, 1993), and later modified by Schwartz (Schwartz, 1994), whereas we in the table in addition include the nomenclature suggested by Ballesteros & Weinstein (Ballesteros and Weinstein, 1995)

MOL 35543

Materials and Methods

Materials. CCR1, -2, CXCR1, -2, -4 and CX3CR1 were kindly provided by Timonthy NC Wells, Serono Pharmaceuticals. CCR3, -4, -6, -9, -10 and -11 were purchased from Origene, www.cDNA.org. CXCR5 and CCR7 were kindly provided by Martin Lipp, MDC-Berlin, Germany. CXCR3 was kindly provided by Kuldeep Neote, Pfizer, Groton, US. XCR1 and CCR8 were kindly provided by Hans R. Lüttichau, Copenhagen University. The human chemokines were purchased from PeproTech (www.peprotech.com) or from R&D (www.RNDsystems.com). The promiscuous chimeric G-protein G α Δ6qi4myr (abbreviated Gqi4myr) was kindly provided by Evi Kostenis (7TM-Pharma, Denmark). ³H-*myo*-inositol and ¹²⁵I-CCL1 were from Amersham Pharmacia Biotech (Uppsala, Sweden). LMD-009 was provided by Millennium Pharmaceuticals.

Site-directed Mutagenesis. The human CCR8 was inserted into the pTEJ8 eukaryotic expression vector or into the FLAG-pcDNA3.1 vector kindly provided by Kate Hansen (7TM-Pharma) and all mutations were done by site-directed mutagenesis using the *Pfu* polymerase (Stratagene). The mutations were verified by DNA sequencing on an ABI 310 sequencer from Perkin-Elmer Inc.

Transfections and tissue culture. COS-7 cells were grown at 10% CO₂ and 37°C in Dulbecco's modified Eagle's medium with glutamax (Gibco, Cat. No 21885-025) adjusted with 10% FBS (fetal bovine serum), 180 u/ml penicillin and 45 ug/mL streptomycin (PenStrep). Transfection of the COS-7 cells was performed by the calcium phosphate precipitation method (Rosenkilde et al., 1999). L1.2 cells stably expressing CCR8 (human or murine) were grown in 6% CO₂ and 37°C in RPMI based medium supplemented with 10% FBS (fetal bovine serum), 180 u/ml penicillin and 45 ug/mL streptomycin (PenStrep). The density of the cell suspension was maintained around 0.7 to 1.0 million cells per ml. Cells were removed from the culture after about 2 months and replaced with freshly thawed cells of lower passage number.

MOL 35543

Inositol-phosphate accumulation (IP-accumulation). COS-7 cells were transfected according to the procedure mentioned above. Briefly, 2×10^6 cells were transfected with receptor or vector control cDNA (from 20 $\mu\text{g}/\text{flask}$) together with 30 μg of the promiscuous chimeric G-protein, Gqi4myr, which turns the $G\alpha_i$ coupled signal into the $G\alpha_q$ pathway (phospholipase C activation measured as IP-accumulation) (Kostenis, 2001) One day after transfection, COS-7 cells (1.5×10^4 cells/well) were incubated for 24 hours with 2 μCi of ^3H -myo-inositol in 0.4 ml growth medium per well. Cells were washed twice in 20 mM HEPES, pH 7.4, supplemented with 140 mM NaCl, 5 mM KCl, 1 mM MgSO_4 , 1 mM CaCl_2 , 10 mM glucose and 0.05% (w/v) bovine serum albumin; and were incubated in 0.4 ml buffer supplemented with 10 mM LiCl for 15 minutes. The ligands were subsequently added and incubated for 90 min. During the antagonist test, the LMD-009 compound was given 15 minutes before the endogenous agonist in order to ensure proper interaction of the receptors with LMD-009. Cells were extracted by addition of 1 ml 10 mM Formic acid to each well followed by incubation on ice for 30-60 min. The generated [^3H]-inositol phosphates were purified on AG 1-X8 anion-exchange resin. Determinations were made in duplicates.

Competition binding experiments. L1.2 cells stably expressing human CCR8 or murine CCR8 were split to 0.5 millions/ml the day before the binding experiments. N-butyric acid to a final concentration of 5 mM was added into the cell suspension (1:100 dilution) in late afternoon. Next day, the cells were harvested by 5 minutes spinning (1350 rpm) and washed once with binding buffer (1xHBSS without phenol red, 0.1% BSA, 0.02% NaN_3), followed by a resuspension in binding buffer at 2 millions cells/ml. 50 μL of the L1.2-CCR8 cell suspension was added into each well of the compound plate (100,000 cells/well), and pipette up and down three times to mix. The unlabeled ligands were in the range from 0.1 nM to 100 μM , and 100 nM unlabeled CCL1 was used as a background control. The cells were incubated with the compounds for 40 min. at room temperature. 50 μL of a 0.2 nM ^{125}I -CCL1 was added to each well and incubated at room temperature for one hour. 100 μL of 0.33% PEI solution was added into each well of a

MOL 35543

filter plate (GF/B), and incubated for about half an hour at room temperature. The samples were harvested using Packard cell harvester, the plates were washed with 4 wells of cold assay wash buffer, the harvester was opened, and the plate was dried under vacuum for about 30 seconds. The filter plate was then air-dried overnight, the plates were bottom-sealed, 500 μ L MicroScint-20 fluid was added to each well, and the top of the plate sealed using Topseal. The plate was read on a topcounter. Determinations were made in quadruplicates

Chemotaxis experiments. The stably transfected L1.2 cells were grown overnight at $0.7-1 \times 10^6$ cells/ml in fresh media. The cells were counted and centrifuged at low speed (~ 1200 RPM) and re-suspended in an equal volume of warm chemotaxis buffer (RPMI medium containing 0.5 % BSA), centrifuged again, aspirated and re-suspended at 1.0×10^7 cells/ml in warm chemotaxis buffer. Chemotaxis was measured using 24 Transwell Polycarbonate 3 μ m Membranes (Corning Costar, Cambridge MA). The bottom wells were filled with increasing concentrations of LMD-009 or CCL1 diluted in 0.6 ml chemotaxis buffer. Chemotaxis plates were then incubated for 4 hours at 37°C in a 5% CO₂-humidified incubator. Following incubation, the cells from the bottom well were collected and counted manually or by a fluorescence-activated cell sorter (FACS Callibur, Becton Dickinson, Franklin Lakes, NJ). Samples were assayed in duplicate.

FLIPR - Calcium mobilization assay. CHO/Ga16 cells stably expressing human CCR8 were plated on 384-well plates (Falcon) at a density of 4×10^3 cells/well and cultured for 2 days at 37 °C and 5 % CO₂. On the third day the cells were incubated with Fluo-3TM (5 μ M) for 1 h (37 °C, 5 % CO₂) and excess dye was removed by extensively washing the cells. To measure the potency of CCR8 agonists to induce intracellular Ca²⁺, plates were loaded onto a Fluorometric Imaging Plate Reader (FLIPR2TM, Molecular

MOL 35543

Devices Inc., Sunnyvale, CA). Ca^{2+} -flux was induced by adding increasing amounts of CCL1, LMD-009 or DMSO only (negative control). EC_{50} values were calculated using XLFit 4.0TM (IDBS, UK).

Surface Enzyme-Linked Immunosorbent Assay (ELISA):

COS-7 cells were transiently transfected with the N-terminal FLAG-tagged variants of CCR8. The cells were washed once in TBS (50 mM Tris-base, 150 mM NaCl, pH 7.6), fixed in 4% glutaraldehyde for 15 min following three washes in TBS and incubation in blocking solution (2% bovine serum albumin in TBS) for 30 min at room temperature. The cells were subsequently incubated 2 hours with anti-FLAG (M1) antibody (2 $\mu\text{g}/\text{ml}$) in TBS supplemented with 1% bovine serum albumin and 1 mM CaCl_2 at room temperature. After three washes in TBS with 1 mM CaCl_2 the cells were incubated with goat anti-mouse horseradish peroxidase-conjugated antibody in the same buffer as the anti-FLAG antibody for 1 h. After three washes in TBS supplemented with 1 mM CaCl_2 the immune reactivity was revealed by the addition of horseradish peroxidase substrate according to manufacture's instruction.

Molecular Modeling. A model of the transmembrane helical bundle of the CCR8 receptor was created using SWISS-MODEL GPCR mode (Schwede et al., 2003). To explore the energy landscape of LMD-009 and find the lowest energy conformation a simulated annealing of LMD-009 was performed. This low energy conformation of LMD-009 was manually docked into the binding pocket of CCR8 using the mutational study results. LMD-009 and the residues in close proximity of the ligand were subsequently minimized while making sure that the initial conformation of the receptor or LMD-009 was not changed considerably.

Calculations. IC_{50} and EC_{50} values were determined by nonlinear regression by using the Prism version 3.0 software (GraphPad Software, San Diego). K_i was calculated using the formula $\text{K}_i = \text{IC}_{50} - [\text{L}]$, where $[\text{L}]$ represents the concentration of applied radioligand.

MOL 35543

Results

Identification of a potent non-peptide CCR8 receptor agonist. In an effort to identify specific non-peptide antagonists for CCR8, we identified an efficacious and potent CCR8 agonist, LMD-009 (Fig. 1A). Comparison of the structure of LMD-009 with the recently disclosed CCR8 agonist, ZK 756326 from Berlex Biosciences (Haskell et al., 2006), revealed structural similarity. However, LMD-009 activated human CCR8 with about 20-fold higher potency. In transiently transfected COS-7 cells expressing the human CCR8 receptor, we measured the ability of LMD-009 to stimulate inositol phosphate accumulation. This assay is based upon a co-transfection with the promiscuous Gqi4myr (a chimeric G α -subunit that is identified as a G α i subunit by the 7TM receptor, but transduces a G α q signal upon activation (Kostenis, 2001)). Under these experimental settings, we observed a potency of LMD-009 that was rather similar to CCL1 (EC₅₀ of 11 nM and 8.7 nM, respectively (Fig.2A)). Given the artificial signalling experiments described above being dependent upon the presence of a chimeric promiscuous G-protein, we decided in addition to use more natural signalling pathways in other cell-lines, hereunder the lymphocyte cell-line L1.2. We therefore tested the ability of LMD-009 to mediate calcium release in CHO-cells and to induce cell migration in the lymphocyte L1.2 cells. Consistent with the data observed from the IP-accumulation assay (Fig. 2A), we observed the same efficacy for LMD-009 and CCL1 in the calcium release experiments (Fig. 2B) and in the chemotaxis experiments (Fig. 2C) – i.e. LMD-009 is a full agonist. In the calcium release experiments we observed a potency (EC₅₀) of 87 ± 17 nM and a Hill-coefficient of 1.39 ± 0.15 for LMD-009 (Fig. 2B).

Many non-peptide antagonists in the chemokine system act as allosteric ligands in respect of showing low affinity in competition binding experiments (see for instance (Watson et al., 2005; Rosenkilde and Schwartz, 2006)). However, in stably transfected L1.2 cells we observed an affinity (K_i) of 66 nM for

MOL 35543

LMD-009 and a complete displacement of all specifically bound ^{125}I -CCL1 (Fig. 2D). That is, the observed binding affinity for LMD-009 is comparable to its potency (Fig. 2).

LMD-009 activates only CCR8 among human chemokine receptors. All the generally accepted human CC, CXC, XC, and CX3C-receptors were screened in order to probe the specificity of the LMD-009 compound. Thus, by measuring IP-accumulation in transiently transfected COS-7 cells (co-transfected with Gqi4myr as above) we observed that the high potency of LMD-009 for human CCR8 was in fact highly selective, as we did not observe any high-potency activation for any of the 17 tested endogenous chemokine receptors. In fact, we did not observe any activation by LMD-009 at concentrations up to 1 μM for CCR2-10, CXCR1-6 and CX3CR1, whereas CCR1 and XCR1 were activated to a slight degree at 1 μM . For all tested receptors, the effect of the endogenous ligand is shown as a positive control (Fig. 3). We also included CCR11 in our test and observed no activation by LMD-009, yet since no agonist has been identified for this receptor, we excluded it from Fig. 3. The recently de-orphanized CXCR7 receptor (previously called RDC-1) was also tested and again no activation by LMD-009 was observed. Yet, since we could not detect any activation with the proposed endogenous ligands for CXCR7 (CXCL11 and CXCL12), we have also excluded this receptor from Fig. 3. Inter-species variations in activity of non-peptide ligands are critical for the valid analysis of these compounds in animal models. In particular, the activity of compounds on the murine homologs is important due to the many murine models of inflammation. We therefore tested the activity of LMD-009 in L1.2 cells stably expressing mouse CCR8 and observed a dose-dependent activation with the same efficacy as TCA-3 (the murine homolog of CCL1), albeit with an 8.5- and 15-fold lower potency, i.e. an EC_{50} of 740 and 580 nM for calcium release and chemotaxis, respectively (data not shown). A similar inter-species difference was found for the recently published ZK756326, that acted with a 10-fold lower potency on murine versus human CCR8 (Haskell et al., 2006). Greater species selectivity (>100-fold between rodent and non-rodent receptors) has

MOL 35543

been observed for other CC and CXC-receptor non-peptide compounds such as the CCR1 antagonist BX471 (R-N-[5-chloro-2-[2-[4-[(4-fluorophenyl)methyl]-2-methyl-1-piperazinyl]-2-oxoethoxy]phenyl]-urea) (Horuk et al., 2001).

Molecular interaction of LMD-009 with CCR8 – GluVII:06 is an anchor-point also for non-peptide agonists. Non-peptide antagonists against CC-chemokine receptors usually share a common pharmacophore with a rather centrally located, positively charged amine (Seibert et al., 2006; Rosenkilde and Schwartz, 2006). This amine has been shown to interact with a highly conserved Glu in the extracellular end of TM-VII (in position VII:06), whereas the flanking groups have been shown to interact with conserved aromatic residues, as well as other residues specific for each chemokine receptor (de Mendonca et al., 2005; Mirzadegan et al., 2000; Maeda et al., 2006; Seibert et al., 2006; Castonguay et al., 2003; Tsamis et al., 2003). Thus, all CC-chemokine receptor non-peptide antagonists with characterized binding modes interact with GluVII:06 (except for the recently characterized binding pocket of BX471 in CCR1 (Vaidehi et al., 2006)) in addition to aromatic residues in the major binding pocket (comprised of TM-III, -IV, -V, -VI and -VII) and in the minor binding pocket (comprised of TM-I, -II, -III, and -VII) (Fig. 1A) (de Mendonca et al., 2005; Mirzadegan et al., 2000; Maeda et al., 2006; Seibert et al., 2006; Castonguay et al., 2003; Tsamis et al., 2003). Like most chemokine receptor non-peptide ligands, LMD-009 contains a positively charged amine (the piperidine-ring of the spiro system). We therefore tested the ability of LMD-009 to activate a mutant form of CCR8 where GluVII:06 was substituted by Ala [E286A]. In this mutation LMD-009 displayed a nearly 1000-fold decreased potency (Table 1, Fig. 4), whereas the endogenous chemokine CCL1 was unaffected. Thus, the non-peptide agonist LMD-009 resembles the majority of CC-chemokine non-peptide antagonists in requiring interaction with GluVII:06.

Position VII:06 is located in the passage between the major and minor binding pockets (Fig. 1). In this inter-face region between TM-III and VII, we mutated three other residues in TM-VII: HisVII:03 (His²⁸³)

MOL 35543

located almost one helical turn above GluVII:06 facing towards the minor binding pocket, SerVII:09 (Ser²⁸⁹) located almost one helical turn below GluVII:06 facing towards the major binding pocket and PheVII:10 (Phe²⁹⁰) located one helical turn below GluVII:06 (Fig. 1). Surprisingly, despite the close proximity to GluVII:06, Ala substitutions at these three positions had no impact on the binding of LMD-009 or CCL1 (Table 1). In TM-III, ValIII:04 (Val¹⁰⁹) is located in close proximity to GluVII:06, yet we observed no change in the potency of LMD-009 or CCL1 upon substitution of ValIII:04 to Ala (Table 1).

Aromatic residues in both the minor and the major ligand-binding pockets are important for the action of LMD-009. Several aromatic residues located at positions in the minor and major ligand-binding pocket, which previously have been described as “hits” (ie. residues of importance) for non-peptide *antagonist* targeting the CCR1, -2, and -5 receptors, were also identified as “hits” for the non-peptide CCR8 *agonist*. Thus in the *minor* binding pocket the Ala substitution of TyrI:07 (Tyr⁴²) resulted in a 15-fold decrease in potency for LMD-009, whereas CCL1 was unaffected (Table 1). Similarly, Ala substitution of PheII:17 (Phe⁸⁸), resulted in a 10-fold decrease in potency for LMD-009, again with no effect on CCL1 (Table 1). In contrast, PheII:13 (Phe⁸⁴) one helical turn below PheII:17 had no impact on the interaction of LMD-009 or CCL1 with CCR8 (Table 1). The Gln residue at position II:20 (Gln⁸¹) is unique for CCR8 among chemokine receptors (85% of endogenous chemokine receptors have a Trp in this position). We substituted Gln with Trp [Q91W] to induce steric hindrance and to make CCR8 more similar to the other CC-chemokine receptors. In contrast to the dependency for a Trp in position II:20 observed for CCR5 non-peptide antagonists (Maeda et al., 2006; Seibert et al., 2006), we observed that both LMD-009 and CCL1 required a small and non-aromatic residue at this position. Thus, the potencies of LMD-009 and CCL1 were decreased by 10- and 7.9-fold, respectively, for the [Q91W] substitution (Table 1, Fig. 6). Not all aromatic residues in this minor pocket were important for the binding of LMD-009, since we observed an unchanged, high potency for LMD-009 and for CCL1 for the Phe III:07 (Phe¹¹²) to Ala and the

MOL 35543

PheIII:18 (Phe¹²³) to Ala substitutions. These positions both face more toward TM-II than toward the minor binding pocket and are both located relatively deep, which could explain the lack of involvement.

In the *major* binding pocket we found that the highly conserved TyrIII:08 (Tyr¹¹³) was essential for the action of LMD-009 as a nearly 1000-fold decrease in potency was observed for the [Y113A] substitution, and that also CCL1 was affected by this mutation with a 37-fold decrease in potency (Table 1, Fig. 5). This was not surprising, as this position is involved in the action of most CCR1,-2, and -5 non-peptide antagonists as well (see discussion). TM-VI contains two highly conserved aromatic residues, TrpVI:13 (Trp²⁵¹) - being part of the conserved “CWLP”-motif (Schwartz et al., 2006) and PheVI:16 (Phe²⁵⁴). We found that the TrpVI:13 was replaceable for the high potency of both LMD-009 and CCL1 based on two different substitutions - [W251A] and [W251Q] (Table 1, Fig. 5 and 6). The [W251Q] substitution was created because some chemokine receptors (CCR6,-7,-9,-11, and CXCR6) have a Gln instead of the otherwise highly conserved Trp in this position (see discussion). The PheVI:16, which is located one helical turn above TrpVI:13, revealed a highly surprising phenotype upon substitution to Ala [F254A] with a 19-fold improvement of LMD-009 potency combined with an increase also in the efficacy for the non-peptide agonist relative to the endogenous CCL1 chemokine (Fig. 5). Thus, LMD-009 acted as a superagonist on the [F254A] mutant form of CCR8. In contrast, CCL1 displayed a 13-fold decrease in potency. One and two helical turns above PheVI:16, we substituted the LeuVI:20 (Leu²⁵⁸) and SerVI:24 (Ser²⁶²) with Ala - [L258A] and [S262A], respectively. Both of these residues – like TrpVI:13 and PheVI:16 – face towards the major binding pocket. However, we did not observe any changes in the potency and efficacy of LMD-009 and CCL1 for the [L258A] and [S262A] mutations (Table 1, Fig. 6). Thus, in the major binding pocket only TyrIII:08 was a classical mutational hit for the LMD-009-mediated activation of CCR8. But the almost 20-fold gain-of-function in respect of potency for LMD-009 observed upon Ala substitution of PheVI:16 indicates a close proximity of part of the non-peptide to this position in CCR8. Both of these mutations impaired the action of CCL1 to the same extent.

MOL 35543

Residues in TM-III, -IV and -V facing into the major binding pocket. Most of these residues are more polar and non-aromatic except for TyrIII:09 (Tyr¹¹⁴) and TyrIV:24 (Tyr¹⁷²). A Tyr in position III:09 is also found in CCR1 where it recently was shown to be important for the binding of the non-peptide antagonist BX471 (Vaidehi et al., 2006). However, we observed only a minor decrease in the potency of LMD-009 (3.9-fold) for the TyrIII:09 to Ala substitution, whereas the potency of CCL1 was decreased 15-fold (Table 1). Position IV:24 has been shown to be involved in the binding of Amlaviroc to CCR5 (Maeda et al., 2006); however, we observed no change in the potency of LMD-009 or CCL1 for the Ala substitution in this position (Table 1). SerIII:05 (Ser¹¹⁰) was changed to Ala, His and Trp, and whereas the Ala substitution resulted in a slight increase (5-7-fold) in the potency of LMD-009 as well as CCL1, the steric hindrance approach severely impaired the activation by both agonists (Table 1). A basic residue is found in position V:01 in 50% of all chemokine receptors, and in CCR5 LysV:01 (Lys¹⁹⁵) has been shown to be important for the binding of Amlaviroc (Maeda et al., 2006). This was not the case in CCR8, as we observed no change in the potency of LMD-009 or CCL1 for the corresponding LysV:01 to Ala substitution (Table 1, Fig. 6). Since the tertiary structure of the extracellular end of TM-V is uncertain (Rosenkilde et al., 2006b; Javitch et al., 2002), we mutated a couple of residues presumably located in the adjacent part of extracellular loop 2, Lys¹⁹³ (position V:-02) and the Trp¹⁹⁴ (in position V:-01). These substitutions had no effect on the potency of LMD-009, whereas CCL1 was impaired with a 15-fold decrease in potency for the [W194A] substitution (Table 1). Position V:12 contains a Gly in almost all chemokine receptors; however substitution with Ala at this position (Gly²⁰⁶) had no effect on the potency of LMD-009, while the potency of CCL1 was impaired by 7.7-fold. In contrast, a substitution with Trp in a steric hindrance approach totally abolished receptor activation by both agonists (Table 1), despite measurable receptor surface expression (Fig. 9B).

Binding mode for different LMD compounds. Besides the LMD-009 compound, we included in current study a series of four analogs that all differed from LMD-009 with regard to the “left side”. Thus they all

MOL 35543

contained the methoxyphenoxybenzyl (“right side”), and the centrally-located positively charged piperidine. The “left sides” were either relatively short with a benzoic acid (LMD-584) or a methoxybenzenesulfonamide (LMD-902) or amide-elongated with either a phenyl-4-(pyrrolidin-1-yl)butanamide (LMD-268) or a oxoquinoline-4-carboxamide (LMD-174) (Fig. 7). The 4 compounds were all probed to the generated CCR8 mutation library as for LMD-009 using the same functional assay with stimulation of IP-accumulation. Interestingly, only very few mutations turned out to affect the non-peptides differently (Fig. 7, Table 2). Thus, neither of four analogs differed from LMD-009 in respect of receptor recognition in the minor binding pocket since they were all affected by the same mutations. i.e. [Y42A] (4.6 to 19 fold decrease in potency), [F88A] (3.1 to 14 fold decrease in potency) and [Q91W] (6.7 to 18 fold decrease in potency). In contrast, the mutations in the major binding pocket affected the compounds with a remarkable and more diverse pattern compared to LMD-009, although the dependency for TyrIII:08 was similar high as for LMD-009. Thus, the improved potency for LMD-009 in the PheVI:16 substitution to Ala [F254A] was not identified for any of the analogs, as the potencies of LMD-584 and LMD-902 were 9.7- and 5.5-fold impaired, respectively, whereas the two amide-elongated compounds were unaffected. The TyrIII:09 to Ala substitution did not affect LMD-009 (Table 1); however we observed impairment of all four analogs for [Y114A]. Thus, the potencies of LMD-584 and of LMD-902 were 15 and 13 fold impaired, whereas the potencies of the two amide-elongated compounds were even more impaired (64 and 31 fold decrease in potency for LMD-268 and LMD-009, Fig. 7). Two of the four compounds (LMD-584 and LMD-902) were in addition impaired by the Ala substitution of LeuVI:20 with a 12 and 7.2-fold decrease in potency, and in addition LMD-584 was affected by the SerVII:09 substitution to Ala with a 7.4-fold impaired potency. Thus, all these differences in the impact of the mutations in the major binding pocket clearly indicate that the “left side” of the compounds is located in this part of the main-binding pocket and that the “right side” is located in the minor binding pocket with the GluVII:06 /piperidine interaction as bridge.

MOL 35543

Molecular modeling of the interaction of LMD-009 with CCR8. A model of the transmembrane helices of CCR8 was created based on an alignment with the bovine rhodopsin crystal structure (Palczewski et al., 2000). Interestingly, the residues identified by mutagenesis studies as being important for CCR8 activation by LMD-009 (Fig. 4-6 and Table 1) were all located at the same level in the receptor (Fig. 8A). A simulated annealing of LMD-009 was performed in order to explore the energy landscape of LMD-009 and to find the lowest energy conformation (data not shown). This low energy conformation of LMD-009 was manually docked into the binding pocket in CCR8 identified by the mutagenesis studies using the presumed interaction of the positively charged amine with the negatively charged carboxylic group of GluVII:06 as a major docking point. LMD-009 and the residues in close proximity to it were subsequently minimized while ensuring that the initial conformation of the receptor and LMD-009 was not changed considerably. Using this approach, LMD-009 could be positioned to make potential interactions with all the identified contact residues (Fig. 8) The methoxyphenoxybenzyl group (in the “right side” of LMD-009, Fig. 1) was positioned into the minor binding pocket (i.e. between TM-I, -II, -III and -VII) with the two benzene rings having favorable hydrophobic interactions with TyrI:07 and PheII:17, respectively (Fig. 8C). The aromatic phenethylimidazoline-4-one (the “left side” of LMD-009) was placed in the major binding pocket (between TM-III, -VI and -VIII) in close proximity to Tyr III:08. The major gain of LMD-009 function for the PheVI:16 to Ala [F254A] mutation was further explored by construction of a computer model of the helical bundle of the [F254A]-CCR8 receptor (Fig. 8D). Using a similar docking approach as presented above - but allowing for further rotation of the phenethyl group at the “left side” of LMD-009 - it was possible to dock this side-chain moiety of the non-peptide agonist into the small, deep cavity, which was created between TM-VI and VII by the PheVI:16 to Ala mutation in the receptor (Fig. 8D). This “improved fit” docking of LMD-009 could potentially represent the structural basis for the observed gain-of-function for this compound in the PheVI:16 to Ala mutation (Fig. 5H).

MOL 35543

Receptor expression versus receptor activity. Among the 29 mutations we observed huge changes in basal and/or agonist-stimulated activity for some (Table 1, Fig. 9A). Thus, while some mutations resulted in large increases in basal (or agonist stimulated) activity, other resulted in the opposite. We therefore decided to N-terminal FLAG-tag a selection of these receptors chosen among the mutations with changed activity levels compared to CCR8 wt in order to determine receptor expression based on a surface Enzyme-Linked Immunosorbent Assay (ELISA, Fig. 9B). Mutations in four aromatic residues resulted in the largest increase in basal activity, with the Ala substitution of PheVII:10 [F290A] resulting in the highest constitutive activity, followed by the Ala substitution of TyrIV:24 [Y172A], the Ala/Gln substitutions of TrpVI:13 [W251A/Q] and the Ala substitution of PheII:13 [F84A]. Importantly, these increases were not followed by corresponding increases in the receptor expression levels (Fig. 9B). In contrast, the decreases in basal and agonist-stimulated activity for His/Trp substitution of SerIII:05 and of Ala/Trp substitution of GlyV:12 were in fact correlated with a remarkably lower surface expression. Among these four mutations, we could only measure the efficacy for [G206A], since the agonist potencies for the three other mutations were decreased to an extent that prevented saturation (no plateau was reached in the dose-response curves, Table 1).

LMD-009 is not an antagonist for other human chemokine receptors. Due to the similarities in the pharmacophore of LMD-009 with many CC-chemokine receptor antagonists (Seibert et al., 2006; Rosenkilde and Schwartz, 2006; de Mendonca et al., 2005; Mirzadegan et al., 2000; Maeda et al., 2006; Seibert et al., 2006; Castonguay et al., 2003; Tsamis et al., 2003) as described above, it was tempting to believe that LMD-009 in fact would act as an antagonist for other CC-chemokine (or maybe even CXC-chemokine) receptors. We therefore repeated the activity screen of LMD-009, this time as antagonist. Thus, the different receptors were activated with submaximal concentrations (from 40-80% stimulation) of the different respective endogenous chemokines, and the putative antagonistic properties of LMD-009 were tested with the results that none of the receptors were inhibited by LMD-009 (Fig. 10).

MOL 35543

Discussion

In the present study we identify a highly potent and selective CCR8 *non-peptide agonist*, LMD-009, and describe its molecular interaction with CCR8 by combining receptor mutagenesis with studies of different chemical analogs of LMD-009. This is to our knowledge the first time the molecular interaction of a *non-peptide agonist* with a chemokine receptor is described. Importantly, we show that the action of LMD-009 (and of the four analogs) depend upon several broadly distributed residues in common with known CC-chemokine receptor *antagonists*, e.g. the highly conserved GluVII:06 in the passage between the major and minor binding pocket, the TyrIII:08 in the major binding pocket and the TyrI:07 and PheII:17 in the minor binding pocket.

Chemokine receptor interaction of non-peptide antagonists versus non-peptide agonists. From a structural point of view, the majority of small molecule non-peptide ligands for CC-chemokine receptors are relatively elongated structures characterized by one (or two) positively charged nitrogen atom(s) located more-or-less centrally in the molecule (Rosenkilde and Schwartz, 2006). Non-peptide *antagonists* following this simplified “pharmacophore model” have almost all been shown to interact with the GluVII:06 via the positively charged nitrogen (Rosenkilde and Schwartz, 2006). However, recently, an elegant study in CCR1 showed that the non-peptide antagonist, BX471 was not dependent upon GluVII:06 but instead interacted with aromatic residues on each side of it, TyrI:07, TyrII:20 and TyrIII:09 (Vaidehi et al., 2006). GluVII:06 is conserved among chemokine receptors (found in 16 out of 21 receptors) and occurs very rarely in non-chemokine receptors (Rosenkilde and Schwartz, 2006). In the present study, we describe how the non-peptide agonist LMD-009 is dependent upon GluVII:06 in CCR8, presumably through a direct interaction of the spiro-ring with the piperidine, and that the “right side” of the LMD-009 molecule interacts with residues in the minor binding pocket, i.e. TyrI:07 and PheII:17, both located at the same level in the helices as VII:06 (Fig. 8A). The requirement for TyrI:07 has been described for several other non-peptide antagonists targeting CCR1 and -5 (Vaidehi et al., 2006; Tsamis et al., 2003; Seibert et

MOL 35543

al., 2006). Thus, molecular modelling of CCR5 has suggested that TyrI:07 (Tyr³⁷) and TrpII:20 (Trp⁸⁶) constitute a large area of the small molecule interface as being in close proximity to the carboxyl group of GluVII:06 (Seibert et al., 2006).

The “left side” of LMD-009 is suggested to be in close proximity to and dependent upon TyrIII:08 in the major binding pocket as described for almost all characterized CC-chemokine receptor antagonists (de Mendonca et al., 2005; Vaidehi et al., 2006; Berkhout et al., 2003; Castonguay et al., 2003; Maeda et al., 2006) and position III:08 – in the form of an Asp - is also a key-interaction point for the monoamines (Schwartz et al., 2006). The orientation of LMD-009 was mainly provided by studying the four analogs LMD-584, LMD-902, LMD-268 and LMD-174 with variation in the “left side” compared to LMD-009, since they all reacted very different from LMD-009 on mutations in the major binding pocket. Most notable are the effects of the mutations in PheVI:16 and TyrIII:09. Thus, in contrast to the 23-fold increase in the potency of LMD-009 for the substitution of PheVI:17 to Ala, we observed a 5-10 fold decrease for LMD-584 and LMD-902, whereas LMD-268 and LMD-174 were unaffected, and in contrast to LMD-009, all analogs depended on TyrIII:09 with the two “elongated” amide-containing compounds being most affected (>25 fold decrease in potency for LMD-268 and LMD-174). The identified impact of PheVI:16 supports the notion that movement of TM-VI is important for receptor activation (Schwartz et al., 2006; Farrens et al., 1996). We suggest that the [F254A] mutation allows LMD-009 to reach deeper down into the pocket formed between TM-VI and -VII, thereby making an inward movement of TM-VI less restricted, and favouring the active conformation of CCR8 (Schwartz et al., 2006). In contrast, LMD-584 and LMD-902 are directly dependent of PheVI:16, whereas the two “elongated” amide-containing LMD-268 and LMD-174 seem to be located more towards the pocket formed by TM-III and -IV, without any interference or interaction with Phe VI:16.

MOL 35543

TrpVI:13 is highly conserved among rhodopsin-like 7TM receptors (71% contain Trp, 90% contain Trp, Phe or Tyr) and is central for the activation mechanism in certain receptors (Schwartz et al., 2006; Shi et al., 2002). In CCR8, we did not observe any change in the agonist potencies upon mutating this residue and together with the fact, that 6 out of 21 chemokine receptors contain a Gln instead of the Trp, we suggest, that TrpVI:13 may not have the same impact on receptor activation as observed in receptor families with smaller ligands (eg. monoamines and ghrelin). This could be due to the large size (70-80 amino-acids) and proposed superficial receptor interaction of the chemokines.

*Chemokine receptor interaction with **peptide** (chemokine) versus **non-peptide** agonist.* Much effort has been made to describe the molecular mechanism of action of endogenous chemokines with their cognate receptors (Jarnagin et al., 1999; Schwarz and Wells, 2002). The three-dimensional structure of chemokines is well-described and the N-terminus (prior to the two first conserved cysteines) is essential for receptor interaction (Hemmerich et al., 1999; Schwarz and Wells, 2002). However, the molecular interaction with the receptor is not yet known in detail. One prevailing model suggests that the chemokine N-terminus docks into the receptor, while the core of the chemokine interacts with residues in the extracellular loops (Schwarz and Wells, 2002). Among the 29 mutations, we only identified two with selective importance for CCL1, namely [W194A] and [G206], located in the top, and middle of TM-V. This position fits with a putative docking of the N-term of CCL1 into the major binding pocket and thereby being dependent upon these two residues that both are located at the interface to the major binding pocket.

Agonist-prone 7TM receptors. For the majority of 7TM receptors high-throughput screening results in the identification of non-peptide antagonists. Yet, for a small fraction non-peptide agonists, rather than antagonists, appear. Some of these agonist-prone receptors display high constitutive activity (e.g. the ghrelin and melanocortin receptors), whereas others are more silent (e.g. somatostatin receptors) (Schwartz et al., 2006). The agonist-prone nature and the constitutive activity in these receptors are

MOL 35543

presumably determined by specific structural features in the receptors although these have not been identified yet. However, it is very likely that the mobility of TM-VI plays an important role as described in the global toggle switch model (Schwartz et al., 2006). CCR8 is an agonist-prone receptor as judged by the discovery of non-peptide agonists (LMD-compounds and ZK 756326) and by the agonistic nature of the other vice antagonistic HHV8-encoded vCCL2 (Dairaghi et al., 1999). The agonist-prone nature of CCR8 was also supported by the observation, that some of the mutations in the major binding pocket (especially [Y172A], and W251A/Q) and in the minor binding pocket ([F84A], and [F290A]) increased the basal signaling, independently of the surface expression (Table 1, Fig. 9). The impact of these mutations in the major binding pocket (and of [F290A]) is in good agreement with the global toggle switch model (Farrens et al., 1996; Schwartz et al., 2006), and the involvement of TM-II (F84A) in receptor activation has also been described previously for CC-chemokine receptors (Govaerts et al., 2001).

What makes an agonist an agonist? In 7TM receptors the binding sites for small molecule ligands - agonists as well as antagonists - have repeatedly been located in the main ligand-binding pocket between the extracellular ends of the transmembrane helices (Schwartz et al., 2006). Yet, despite the fact that various differences have been described between agonists and antagonists in specific cases, the general molecular mechanism which for some compounds leads to agonism and for others – even rather structurally similar compounds - leads to antagonism, has remained unclear. However, in the CXCR3 receptor, we have recently shown that small and simple compounds – bipyridine or phenanthroline – could be turned into a highly efficacious agonist by ensuring that it - through an anchoring, silent metal-ion site – is tethered at a position corresponding to the binding site for β 2-adrenergic agonists, i.e. between TM-III, -IV and -V (Rosenkilde et al., 2006a). All together, these efficient non-peptide agonists (in for instance CXCR3 and CCR8) are important tools for the elucidation of the mechanism of receptor activation, a prerequisite for rational design of efficient non-peptide antagonists for 7TM-receptors.

MOL 35543

In the present study we find that the small molecule agonist LMD-009, like small molecule antagonists in chemokine receptors in general, uses GluVII:06 as a major anchor-point to interact with mainly aromatic key residues on each side, i.e. in the minor and major ligand-binding pocket, respectively. LMD-009 appears to bind relatively superficially in the pocket (Fig. 8A). Such a binding mode is in agreement with recent observations in the ghrelin receptor where small peptide-based agonists also interact superficially in the corresponding area of the receptor, whereas compounds where minor modification in the ligands allow for a deeper anchorage in the binding pocket are antagonists (Holst et al., 2006). It will therefore be extremely interesting to map the receptor binding sites of the recently published CCR8 small molecule antagonists (Ghosh et al., 2006) in the near future.

Acknowledgements – Lisbet Elbak, Randi Thøgersen and Inger Smith Simonsen are thanked for excellent and skilful technical assistance. Laura Storjohann is thanked for critical reading and fruitful discussion of the manuscript and Trond Ulven is thanked for chemical support.

MOL 35543

Reference List

- Baldwin JM (1993) The Probable Arrangement of the Helices in G Protein-Coupled Receptors. *EMBO J* **12**:1693-1703.
- Ballesteros JA and Weinstein H (1995) Integrated methods for the construction of three-dimensional models and computational probing of structure-function relations in G protein-coupled receptors, in *Receptor Molecular Biology* (Sealfon SC ed) pp 366-428, Academic Press, New York.
- Berkhout TA, Blaney F E, Bridges A M, Cooper D G, Forbes I T, Gribble A D, Groot P H, Hardy A, Ife R J, Kaur R, Moores K E, Shillito H, Willetts J and Witherington J (2003) CCR2: Characterization of the Antagonist Binding Site From a Combined Receptor Modeling/Mutagenesis Approach. *J Med Chem* **46**:4070-4086.
- Castonguay LA, Weng Y, Adolfsen W, Di Salvo J, Kilburn R, Caldwell C G, Daugherty B L, Finke P E, Hale J J, Lynch C L, Mills S G, MacCoss M, Springer M S and DeMartino J A (2003) Binding of 2-Aryl-4-(Piperidin-1-Yl)Butanamines and 1,3,4-Trisubstituted Pyrrolidines to Human CCR5: a Molecular Modeling-Guided Mutagenesis Study of the Binding Pocket. *Biochemistry* **42**:1544-1550.
- Chensue SW, Lukacs N W, Yang T Y, Shang X, Frait K A, Kunkel S L, Kung T, Wiekowski M T, Hedrick J A, Cook D N, Zingoni A, Narula S K, Zlotnik A, Barrat F J, O'Garra A, Napolitano M and Lira S A (2001) Aberrant in Vivo T Helper Type 2 Cell Response and Impaired Eosinophil Recruitment in CC Chemokine Receptor 8 Knockout Mice. *J Exp Med* **193**:573-584.
- Dairaghi DJ, Fan R A, McMaster B E, Hanley M R and Schall T J (1999) HHV8-Encoded VMIP-I Selectively Engages Chemokine Receptor CCR8. Agonist and Antagonist Profiles of Viral Chemokines. *J Biol Chem* **274**:21569-21574.
- Damon I, Murphy P M and Moss B (1998) Broad Spectrum Chemokine Antagonistic Activity of a Human Poxvirus Chemokine Homolog. *Proc Natl Acad Sci* **95**:6403-6407.
- de Mendonca FL, da Fonseca P C, Phillips R M, Saldanha J W, Williams T J and Pease J E (2005) Site-Directed Mutagenesis of CC Chemokine Receptor 1 Reveals the Mechanism of Action of UCB 35625, a Small Molecule Chemokine Receptor Antagonist. *J Biol Chem* **280**:4808-4816.
- Farrens DL, Altenbach C, Yang K, Hubbell W L and Khorana H G (1996) Requirement of Rigid-Body Motion of Transmembrane Helices for Light Activation of Rhodopsin. *Science* **274**:768-770.
- Gerard C and Rollins B J (2001) Chemokines and Disease. *Nat Immunol* **2**:108-115.
- Ghosh S, Elder A, Guo J, Mani U, Patane M, Carson K, Ye Q, Bennett R, Chi S, Jenkins T, Guan B, Kolbeck R, Smith S, Zhang C, LaRosa G, Jaffee B, Yang H, Eddy P, Lu C, Uttamsingh V, Horlick R, Harriman G and Flynn D (2006) Design, Synthesis, and Progress Toward Optimization of Potent Small Molecule Antagonists of CC Chemokine Receptor 8 (CCR8). *J Med Chem* **49**:2669-2672.
- Govaerts C, Blanpain C, Deupi X, Ballet S, Ballesteros J A, Wodak S J, Vassart G, Pardo L and Parmentier M (2001) The TXP Motif in the Second Transmembrane Helix of CCR5. A Structural Determinant of Chemokine-Induced Activation. *J Biol Chem* **276**:13217-13225.

MOL 35543

Haskell CA, Horuk R, Liang M, Rosser M, Dunning L, Islam I, Kremer L, Gutierrez J, Marquez G, Martinez A, Biscone M J, Doms R W and Ribeiro S (2006) Identification and Characterization of a Potent, Selective Nonpeptide Agonist of the CC Chemokine Receptor CCR8. *Mol Pharmacol* **69**:309-316.

Hemmerich S, Paavola C, Bloom A, Bhakta S, Freedman R, Grunberger D, Krstenansky J, Lee S, McCarley D, Mulkins M, Wong B, Pease J, Mizoue L, Mirzadegan T, Polsky I, Thompson K, Handel T M and Jarnagin K (1999) Identification of Residues in the Monocyte Chemotactic Protein-1 That Contact the MCP-1 Receptor, CCR2. *Biochemistry* **38**:13013-13025.

Holst B, Lang M, Brandt E, Bach A, Howard A, Frimurer T M, Beck-Sickinger A and Schwartz T W (2006) Ghrelin Receptor Inverse Agonists: Identification of an Active Peptide Core and Its Interaction Epitopes on the Receptor. *Mol Pharmacol* **70**:936-946.

Horuk R (2003) Development and Evaluation of Pharmacological Agents Targeting Chemokine Receptors. *Methods* **29**:369-375.

Horuk R, Clayberger C, Krensky A M, Wang Z, Grone H J, Weber C, Weber K S, Nelson P J, May K, Rosser M, Dunning L, Liang M, Buckman B, Ghannam A, Ng H P, Islam I, Bauman J G, Wei G P, Monahan S, Xu W, Snider R M, Morrissey M M, Hesselgesser J and Perez H D (2001) A Non-Peptide Functional Antagonist of the CCR1 Chemokine Receptor Is Effective in Rat Heart Transplant Rejection. *J Biol Chem* **276**:4199-4204.

Jarnagin K, Grunberger D, Mulkins M, Wong B, Hemmerich S, Paavola C, Bloom A, Bhakta S, Diehl F, Freedman R, McCarley D, Polsky I, Ping-Tsou A, Kosaka A and Handel T M (1999) Identification of Surface Residues of the Monocyte Chemotactic Protein 1 That Affect Signaling Through the Receptor CCR2. *Biochemistry* **38**:16167-16177.

Javitch JA, Shi L and Liapakis G (2002) Use of the Substituted Cysteine Accessibility Method to Study the Structure and Function of G Protein-Coupled Receptors. *Methods Enzymol* **343**:137-156.

Kostenis E (2001) Is Galpha16 the Optimal Tool for Fishing Ligands of Orphan G-Protein-Coupled Receptors? *Trends Pharmacol Sci* **22**:560-564.

Maeda K, Das D, Ogata-Aoki H, Nakata H, Miyakawa T, Tojo Y, Norman R, Takaoka Y, Ding J, Arnold E and Mitsuya H (2006) Structural and Molecular Interactions of CCR5 Inhibitors With CCR5. *J Biol Chem*.

Mirzadegan T, Diehl F, Ebi B, Bhakta S, Polsky I, McCarley D, Mulkins M, Weatherhead G S, Lapierre J M, Dankwardt J, Morgans D, Jr., Wilhelm R and Jarnagin K (2000) Identification of the Binding Site for a Novel Class of CCR2b Chemokine Receptor Antagonists: Binding to a Common Chemokine Receptor Motif Within the Helical Bundle. *J Biol Chem* **275**:25562-25571.

Murphy PM, Baggiolini M, Charo I F, Hebert C A, Horuk R, Matsushima K, Miller L H, Oppenheim J J and Power C A (2000) International Union of Pharmacology. XXII. Nomenclature for Chemokine Receptors. *Pharmacol Rev* **52**:145-176.

Palczewski K, Kumasaka T, Hori T, Behnke C A, Motoshima H, Fox B A, Le T, I, Teller D C, Okada T, Stenkamp R E, Yamamoto M and Miyano M (2000) Crystal Structure of Rhodopsin: A G Protein-Coupled Receptor. *Science* **289**:739-745.

MOL 35543

Rosenkilde MM, Andersen M B, Nygaard R, Frimurer T M and Schwartz T W (2006a) Activation of the CXCR3 Chemokine Receptor Through Anchoring of a Small Molecule Chelator Ligand Between TM-III, -IV and -VI. *Mol Pharmacol*.

Rosenkilde MM, David R, Oerlecke I, ned-Jensen T, Geumann U, Beck-Sickinger A G and Schwartz T W (2006b) Conformational Constraining of Inactive and Active States of a Seven Transmembrane Receptor by Metal Ion Site Engineering in the Extracellular End of Transmembrane Segment V. *Mol Pharmacol* **70**:1892-1901.

Rosenkilde MM, Kledal T N, Brauner-Osborne H and Schwartz T W (1999) Agonists and Inverse Agonists for the Herpesvirus 8-Encoded Constitutively Active Seven-Transmembrane Oncogene Product, ORF-74. *J Biol Chem* **274**:956-961.

Rosenkilde MM and Schwartz T W (2006) GluVII:06 - A Highly Conserved and Selective Anchor Point for Non-Peptide Ligands in Chemokine Receptors. *Curr Top Med Chem* **6**:1319-1333.

Schwartz TW (1994) Locating Ligand-Binding Sites in 7TM Receptors by Protein Engineering. *Curr Opin Biotech* **5**:434-444.

Schwartz TW, Frimurer T M, Holst B, Rosenkilde M M and Elling C E (2006) Molecular Mechanism of 7tm Receptor Activation-a Global Toggle Switch Model. *Annu Rev Pharmacol Toxicol* **46**:481-519.

Schwarz MK and Wells T N (2002) New Therapeutics That Modulate Chemokine Networks. *Nat Rev Drug Discov* **1**:347-358.

Schwede T, Kopp J, Guex N and Peitsch M C (2003) SWISS-MODEL: An Automated Protein Homology-Modeling Server. *Nucleic Acids Res* **31**:3381-3385.

Seibert C, Ying W, Gavrilov S, Tsamis F, Kuhmann S E, Palani A, Tagat J R, Clader J W, McCombie S W, Baroudy B M, Smith S O, Dragic T, Moore J P and Sakmar T P (2006) Interaction of Small Molecule Inhibitors of HIV-1 Entry With CCR5. *Virology* **349**:41-54.

Shi L, Liapakis G, Xu R, Guarnieri F, Ballesteros J A and Javitch J A (2002) Beta2 Adrenergic Receptor Activation. Modulation of the Proline Kink in Transmembrane 6 by a Rotamer Toggle Switch. *J Biol Chem* **277**:40989-40996.

Soler D, Chapman T R, Poisson L R, Wang L, Cote-Sierra J, Ryan M, McDonald A, Badola S, Fedyk E, Coyle A J, Hodge M R and Kolbeck R (2006) CCR8 Expression Identifies CD4 Memory T Cells Enriched for FOXP3+ Regulatory and Th2 Effector Lymphocytes. *J Immunol* **177**:6940-6951.

Trebst C, Staugaitis S M, Kivisakk P, Mahad D, Cathcart M K, Tucky B, Wei T, Rani M R, Horuk R, Aldape K D, Pardo C A, Lucchinetti C F, Lassmann H and Ransohoff R M (2003) CC Chemokine Receptor 8 in the Central Nervous System Is Associated With Phagocytic Macrophages. *Am J Pathol* **162**:427-438.

Tsamis F, Gavrilov S, Kajumo F, Seibert C, Kuhmann S, Ketas T, Trkola A, Palani A, Clader J W, Tagat J R, McCombie S, Baroudy B, Moore J P, Sakmar T P and Dragic T (2003) Analysis of the Mechanism by Which the Small-Molecule CCR5 Antagonists SCH-351125 and SCH-350581 Inhibit Human Immunodeficiency Virus Type 1 Entry. *J Virol* **77**:5201-5208.

MOL 35543

Vaidehi N, Schlyer S, Trabanino R J, Floriano W B, Abrol R, Sharma S, Kochanny M, Koovakat S, Dunning L, Liang M, Fox J M, de Mendonca F L, Pease J E, Goddard W A, III and Horuk R (2006) Predictions of CCR1 Chemokine Receptor Structure and BX 471 Antagonist Binding Followed by Experimental Validation. *J Biol Chem* **281**:27613-27620.

Watson C, Jenkinson S, Kazmierski W and Kenakin T (2005) The CCR5 Receptor-Based Mechanism of Action of 873140, a Potent Allosteric Noncompetitive HIV Entry Inhibitor. *Mol Pharmacol* **67**:1268-1282.

Wells TN, Power C A, Shaw J P and Proudfoot A E (2006) Chemokine Blockers--Therapeutics in the Making? *Trends Pharmacol Sci* **27**:41-47.

MOL 35543

Footnotes

a) The study was supported by the Danish Research Council, and the NovoNordisk Foundation, and the Aase og Einer Danielsen Foundation.

b) Reprint requests to:

Mette M. Rosenkilde, Laboratory for Molecular Pharmacology,

Department of Pharmacology, The Panum Institute, Copenhagen University,

Blegdamsvej 2, 2200 Copenhagen, Denmark,

Phone: 0045 61364871, Fax : 0045 35327610, e-mail: rosenkilde@molpharm.dk

c) Numbered footnotes:

¹ In the text we use the generic 7TM numbering system suggested by Baldwin (Baldwin, 1993), and later modified by Schwartz (Schwartz, 1994), whereas we in the table in addition include the nomenclature suggested by Ballesteros & Weinstein (Ballesteros and Weinstein, 1995)

MOL 35543

Legends for figures

Fig. 1. Helical wheel diagram of CCR8 together with the structures of the two identified CCR8 receptor non-peptide agonists, LMD-009 and ZK 756326. The circles with grey background in the helical wheel diagram indicate mutations performed in the present study. The circles with black background indicate conserved residues within the rhodopsin-like 7TM receptors. The structure of LMD-009 (8-[3-(2-methoxyphenoxy)benzyl]-1-phenethyl-1,3,8-triaza-spiro[4.5]decan-4-one) is shown together with the structure of the recently published CCR8 agonist ZK 756326 (2-[2-[4-(3-Phenoxybenzyl)piperazin-1-yl]ethoxy]ethanol) (Haskell et al., 2006).

Fig. 2. LMD-009 activates CCR8 with high potency and efficacy, and completely displaces ¹²⁵I-CCL1 with high affinity. *Panel A* - The phosphatidyl-inositol (PI)-accumulation experiments were performed in transiently transfected COS-7 cells. Dose-response curves with LMD-009 (□) and CCL1 (●) *Panel B and C* - The Calcium release experiments and the competition binding experiments were performed in stably transfected L1.2 cells. (n=3-63).

Fig. 3. LMD-009 only activates CCR8 among all human chemokine receptors. The IP-accumulation experiments were performed in transiently transfected COS-7 cells. Dose-response curves for LMD-009 (▼) and of the positive controls (■) selected among the possible endogenous chemokine agonists. (n=3-63).

Fig. 4. GluVII:06 is an anchor-point for LMD-009. The IP-accumulation experiments were performed in transiently transfected COS-7 cells. *Panel A* - Dose-response curves for CCL1 on CCR8 wt (□) and [E286A] (■) where 100% equals the maximal stimulation of CCL1 on CCR8 wt. *Panel B* - Dose-response curves for LMD-009 on CCR8 wt (○) and [E286A] (●), where 100% equals the maximal stimulation of CCL1 on each receptor. (n=3-63).

MOL 35543

Fig. 5. CCL1 and LMD-009 depend upon certain aromatic residues in CCR8. The IP-accumulation experiments were performed in transiently transfected COS-7 cells. A selection of aromatic residues mutated into Ala is presented. CCL1 is shown in squares on wt (□) and mutated receptors (■), whereas LMD-009 is shown in circles on wt (○) and mutated receptors (●). *Panel A and B* - Mutation of TyrIII:08 to Ala [Y113A]. *Panel C and D* - Mutation of TyrIII:09 to Ala [Y114A]. *Panel E and F* - Mutation of TrpVI:13 to Ala [W251A]. *Panel G and H* - Mutation of PheVI:16 to Ala [F254A]. *Panel I and J* - Mutation of PheVII:10 to Ala [F290A]. The curves for CCL1 (*A, C, E, G, I*) are all normalized the basal and maximum IP-accumulation on wt receptor, whereas the curves for LMD-009 (*B, D, F, H, J*) are all normalized to the basal and maximum CCL1 induced IP-accumulation on each receptor. (n=3-63).

Fig. 6. Residues identified through mutagenesis to be important for the action of CCL1 and LMD-009 shown in a helical wheel diagram of the CCR8 receptor. The background colors indicate the magnitude of the effect of the mutation on the action of CCL1 (*left panel*) and LMD-009 (*right panel*). Grey background indicates <5-fold decrease in potency, yellow, 5- to 25-fold decrease, orange, 25- to 100-fold decrease, and red, >100-fold decrease in potency. Green background indicates >5-fold increase in potency. The actual potencies are shown in Table 1.

Fig. 7. Residues identified through mutagenesis to be important for the action of LMD-584, LMD-268, LMD-902 and LMD-174 shown in a helical wheel diagram of the CCR8 receptor. The background colors indicate the magnitude of the effect of the mutation on the action of LMD-584 2-(1-(3-(2-methoxyphenoxy)benzyl)-4-hydroxypiperidin-4-yl)benzoic acid, LMD-902 N-ethyl-2-{4-hydroxy-1-[3-(2-methoxyphenoxy)benzyl]piperidin-4-yl}-4-methoxybenzenesulfonamide, LMD-268 N-(1-(3-(2-methoxyphenoxy)benzyl)piperidin-4-yl)-2-phenyl-4-(pyrrolidin-1-yl)butanamide, and LMD-174 N-(1-(3-(2-methoxyphenoxy)benzyl)piperidin-4-yl)-1,2,3,4-tetrahydro-2-oxoquinoline-4-carboxamide. Grey background indicates <5-fold decrease in potency, yellow, 5- to 25-fold decrease, orange, 25- to 100-fold

MOL 35543

decrease, and *red*, >100-fold decrease in potency. Green background indicates >5-fold increase in potency. The actual potencies are shown in Table 2.

Fig. 8. Molecular model of the interaction of LMD-009 with the transmembrane helical bundle of the CCR8 receptor. The CCR8 model was built over the X-ray structure of bovine rhodopsin and a low energy conformation of LMD-009 was generated by simulated annealing (see text for details). *Panel A* – Side view of the helical bundle – shown in blue solid ribbons - of the CCR8 receptor with the residues identified by mutagenesis as presumed interaction points for LMD-009 (Fig. 5, Table 1) shown in stick models and where the ribbons for TM-VI and -VII have been removed in front for better view of the binding site. *Panel B* – Top view from the extracellular side of the model shown in panel A. *Panel C* – Top view of the CCR8 model with the electrostatic surface displayed (negative charge in red and positive charge in blue) where LMD-009 – shown in stick model - has been docked into its presumed binding site. The electrostatic surfaces of the binding pocket is dominated by the negative charge of GluVII:06, which interacts with the positive charged nitrogen of the piperidin ring of LMD-009. The position of the side chains of the presumed contact residues are indicated by yellow labels. *Panel D* – Top view similar to that shown in panel C of a model of the [F254A]-CCR8 construct, which demonstrated a 19-fold gain of function for LMD-009. It is proposed that the phenethyl ring of the “left side” of LMD-009 as shown is able to insert into the pocket generated between TM-VI and -VII through the PheVI:16 to Ala substitution and that this improved fit could be responsible for the gain-of-function in respect of LMD-009 potency observed in the [F254A]-CCR8 construct.

Fig. 9. Receptor activation and receptor expression levels. *Panel A* - Basal receptor activity measured by IP-accumulation for all CCR8 mutations, adapted from Table 1. The mutations depicted in black columns were chosen for FLAG-tagging followed by surface expression determination (ELISA). *Panel B*-

MOL 35543

The ELISA was performed in transiently transfected COS-7 using the same transfection method as for the activity measurements in (A). 100% equals the specific expression of wt CCR8. (n=3).

Fig. 10. LMD-009 is not an antagonist for any human chemokine receptor. The IP-accumulation experiments were performed in transiently transfected COS-7 cells. Dose-response curves for LMD-009 (▼) and of the positive controls (■) selected among the possible endogenous chemokine agonists. The receptors were stimulated with the selected endogenous agonist at sub-maximal concentrations, aiming at 40-80% stimulation, for the antagonist test (n=3).

Table 1. Molecular interaction of CCL1 and LMD-009 with CCR8. The whole panel of CCR8 mutations was screened for the ability of the endogenous chemokine CCL1 (left side panel) and the non-peptide LMD-009 (right side panel) to activate every single mutation. The CCR8 receptors were expressed in transiently transfected COS-7 cells and the activation was measured by means of accumulated phosphatidyl-inositols (PI-accumulation - see Experimental Procedures). The table shows the potency (both as Log EC₅₀ and as EC₅₀) and the level of activation (basal and agonist stimulated levels (efficacy)). The differences between the potency of CCL1 or LMD-009 on a given mutation and the potency of each ligand on wt CCR8 are shown in the columns named "Fold". NE stands for "not estimated due to no plateau", and NA stands for "no activation at all". The numbers of experiments are given as (n). The nomenclature of the receptor residues are given both according to the Schwartz/Baldwin, and the Ballesteros/Weinstein (see footnote 1)

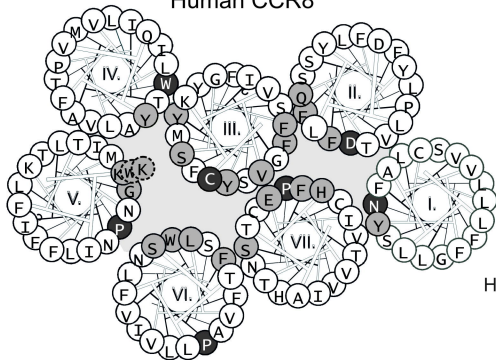
Residue			CCL1									LMD-009						
Position*	Number		Potency			Efficacy			Basal act.			Potency			Efficacy			
Schwartz	Ballesteros Weinstein		EC ₅₀	SEM	EC ₅₀	Fold	(n)	E _{max}	SEM	Basal	SEM	EC ₅₀	SEM	EC ₅₀	Fold	(n)	E _{max}	SEM
			(Log)		(nM)			(cpm)		(cpm)		(Log)		(nM)			(cpm)	
wt	wt	wt	-8.1 ±	0.03	8.7	1.0	(65)	4000 ±	314	712	± 40	-8.0 ±	0.17	11	1.0	(11)	3774 ±	448
I:07	1.39	Y42A	-7.9 ±	0.13	11	1.3	(9)	2238 ±	370	786	± 120	-6.8 ±	0.09	158	15	(3)	1471 ±	302
I:11	1.43	F46A																
II:13	2.53	F84A	-8.4 ±	0.13	4.0	0.46	(8)	2098 ±	278	1009	± 87	-7.9 ±	0.09	14	1.3	(3)	1441 ±	158
II:17	2.57	F88A	-8.0 ±	0.05	10	1.2	(9)	2445 ±	419	799	± 118	-7.0 ±	0.05	108	10	(4)	1107 ±	450
II:20	2.60	Q91W	-7.2 ±	0.14	69	7.9	(6)	1232 ±	101	665	± 58	-7.0 ±	0.18	108	10	(3)	2916 ±	92
III:04	3.28	V109A	-8.1 ±	0.07	8.2	0.95	(3)	2100 ±	356	940	± 269	-8.1 ±	0.21	7.7	0.73	(3)	2193 ±	297
III:05	3.29	S110A	-8.8 ±	0.10	1.6	0.18	(8)	2804 ±	723	861	± 214	-8.8 ±	0.41	1.5	0.14	(4)	1066 ±	596
III:05	3.29	S110W	<-6		>1000	>137	(7)	NE		556	± 850	<-5		>10000	>950	(2)	NE	
III:07	3.31	F112A	-8.3 ±	0.07	4.6	0.53	(9)	3706 ±	552	651	± 88	-7.9 ±	0.04	11	1.1	(4)	2394 ±	702
III:08	3.32	Y113A	-6.5 ±	0.12	323	37	(10)	1047 ±	185	570	± 57	<-5 ±	0.00	>10000	>950	(5)	NE	
III:09	3.33	Y114A	-6.9 ±	0.13	131	15	(4)	2692 ±	784	927	± 200	-7.4 ±	0.09	42	3.9	(6)	3652 ±	710
III:18	3.42	F123A	-8.4 ±	0.15	4.4	0.51	(6)	1466 ±	371	426	± 64	-8.2 ±	0.14	7.0	0.66	(3)	1430 ±	280
IV:20	4.60	L168D	-7.9 ±	0.18	12	1.4	(11)	3549 ±	537	948	± 122	-7.8 ±	0.17	18	1.7	(2)	4410 ±	1576
IV:24	4.64	Y172A	-8.0 ±	0.11	11	1.3	(8)	2000 ±	155	1315	± 110	-7.7 ±	0.15	21	2.0	(4)	1557 ±	329
V:-02	5.33	K193A	-7.7 ±	0.17	22	2.6	(6)	2956 ±	352	659	± 89	-8.1 ±	0.37	8.5	0.80	(2)	3414 ±	298
V:-01	5.34	W194A	-6.9 ±	0.29	128	15	(5)	2500 ±	142	673	± 44	-8.1 ±	0.23	7.6	0.72	(3)	1273 ±	207
V:01	5.35	K195A	-8.1 ±	0.09	7.5	0.87	(7)	1947 ±	314	666	± 97	-8.2 ±	0.30	6.2	0.59	(3)	2370 ±	485
V:12	5.46	G206A	-7.2 ±	0.13	67	7.7	(9)	904 ±	63	508	± 54	-7.7 ±	0.08	19	1.4	(3)	744 ±	59
V:12	5.46	G206W	NA				(8)	501 ±	75	NA		NA				(3)		
VI:13	6.48	W251Q	8.5 ±	0.12	3.4	0.39	(10)	2245 ±	347	1146	± 152	-7.8 ±	0.34	44	4.1	(3)	1112 ±	468
VI:13	6.48	F251Q	-8.2 ±	0.14	6.6	0.76	(6)	2528 ±	320	1097	± 166	-7.4 ±	0.34	44	4.1	(3)	1112 ±	468
VI:16	6.51	F254A	-7.0 ±	0.09	109	13	(10)	3131 ±	609	835	± 74	-9.2 ±	0.24	0.57	0.05	(5)	6640 ±	1484
VI:20	6.55	L258A	-7.6 ±	0.11	27	3.2	(9)	2699 ±	262	591	± 54	-7.9 ±	0.20	13	1.2	(3)	3162 ±	568
VI:24	6.59	S262A	-8.3 ±	0.10	5.2	0.60	(10)	2949 ±	420	621	± 67	-7.7 ±	0.16	21	2.0	(4)	1854 ±	815
VII:03	7.36	H283A	-7.9 ±	0.09	12	1.4	(8)	4003 ±	444	705	± 58	-7.6 ±	0.14	24	2.2	(3)	3644 ±	1595
VII:06	7.39	E286A	-7.9 ±	0.11	12	1.4	(11)	3732 ±	578	930	± 96	<-5		>10000	>950	(5)	NE	
VII:09	7.42	S289A	-7.7 ±	0.14	18	2.1	(3)	9229 ±	3007	842	± 293	-7.8 ±	0.03	16	1.5	(3)	10833 ±	2827
VII:10	7.43	F290A	-8.2 ±	0.20	6	0.68	(5)	4325 ±	940	2497	± 517	-7.7 ±	0.08	20	1.9	(5)	3700 ±	789

Table 2. Molecular interaction of LMD-584, LMD-902, LMD-268 and LMD-174 with CCR8. The whole panel of CCR8 mutations was screened for the ability of the four additional non-peptide agonists to activate every single mutation. The CCR8 receptors were expressed in transiently transfected COS-7 cells and the activation was measured by means of accumulated inositol-phosphates (IP). The table shows the potency (both as Log EC₅₀ and as EC₅₀). The differences between the potency of each compound on a given mutation and the potency of each ligand on wt CCR8 are shown in the columns named "Fold". NA stands for "no activation at all". The numbers of experiments are given as (n). The nomenclature of the receptor residues are given both according to the Schwartz/Baldwin, and the Ballesteros/Weinstein (see footnote 1)

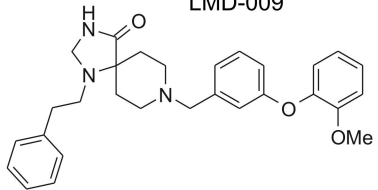
Residue		LMD-584					LMD-902					LMD-268					LMD-174					
Position	Number	EC ₅₀	SEM	EC ₅₀	Fold	(n)	EC ₅₀	SEM	EC ₅₀	Fold	(n)	EC ₅₀	SEM	EC ₅₀	Fold	(n)	EC ₅₀	SEM	EC ₅₀	Fold	(n)	
Schwartz	Bal. We	(Log)		(nM)			(Log)		(nM)			(Log)		(nM)			(Log)		(nM)			
wt	wt	-7.5	± 0.07	29	1.0	(15)	-7.8	± 0.10	15	1.0	(8)	-8.0	± 0.05	9.0	1.0	(4)	-7.5	± 0.05	30	1.0	(15)	
I:07	1.39	Y42A	-6.9	± 0.04	131	4.6	(3)	-6.7	± 0.18	178	12	(3)	-6.8	± 0.22	172	19	(3)	-6.7	± 0.14	199	6.6	(3)
I:11	1.43	F46A	-6.9	± 0.05	126	4.4	(3)	-7.3	± 0.07	50	3.4	(3)	-7.4	± 0.06	43	4.8	(2)	-7.3	± 0.18	52	1.7	(3)
II:13	2.53	F84A	-8.2	± 0.25	7.0	0.24	(4)	-7.9	± 0.03	12	0.85	(3)	-8.3	± 0.06	4.8	0.54	(4)	-6.9	± 0.28	133	4.4	(4)
II:17	2.57	F88A	-6.6	± 0.19	251	8.8	(3)	-6.7	± 0.20	197	14	(4)	-7.5	± 0.23	31	3.5	(3)	-7.0	± 0.05	94	3.1	(3)
II:20	2.60	Q91W	-6.4	± 0.36	368	13	(3)	-6.7	± 0.13	180	12	(3)	-6.8	± 0.25	161	18	(3)	-6.7	± 0.17	201	6.7	(3)
III:04	3.28	V109A	-7.5	± 0.26	34	1.2	(3)	-8.1	± 0.05	8	0.52	(3)	-8.6	± 0.11	2.6	0.29	(3)	-7.5	± 0.18	33	1.1	(3)
III:05	3.29	S110A	-8.2	± 0.38	6.0	0.21	(4)	-8.7	± 0.34	2	0.15	(3)	-8.8	± 0.11	1.6	0.18	(6)	-8.4	± 0.15	3.6	0.12	(4)
III:05	3.29	S110H	<-5		>10000	>323	(3)	<-5	± 0.00	>10000	>689	(2)	<-5		>10000	>1100	(2)	<-5		>10000	>323	(3)
III:05	3.29	S110W	<-5		>10000	>323	(4)	<-5	± 0.00	>10000	>689	(2)	<-5		>10000	>1100	(3)	<-5		>10000	>323	(3)
III:07	3.31	F112A	-7.3	± 0.08	51	1.8	(4)	-7.9	± 0.09	13	0.88	(4)	-8.1	± 0.08	7.1	0.79	(6)	-7.4	± 0.08	37	1.2	(4)
III:08	3.32	Y113A	<-5	± 0.00	>10000	>323	(3)	>-5		>10000	>689	(3)	<-5		>10000	>1100	(3)	<-5	±	>10000	>323	(4)
III:09	3.33	Y114A	-6.4	± 0.32	430	15	(3)	-6.7	± 0.11	191	13	(3)	-6.2	± 0.06	579	64	(3)	-6.0	± 0.11	945	31	(3)
III:18	3.42	F123A	-7.7	± 0.14	21	0.73	(3)	-7.9	± 0.02	12	0.85	(3)	-8.3	± 0.17	5.0	0.56	(5)	-7.7	± 0.07	19	0.63	(3)
IV:24	4.64	Y172A	-7.3	± 0.19	56	1.9	(4)	-7.5	± 0.15	31	2.1	(3)	-7.6	± 0.20	28	3.1	(3)	-7.0	± 0.04	93	3.1	(5)
V:-02	5.34	K193A	-7.5	± 0.18	31	1.1	(4)	-7.8	± 0.52	17	1.2	(2)	-8.3	± 0.17	4.7	0.52	(3)	-7.5	± 0.06	30	1.0	(3)
V:-01	5.33	W194A	-7.9	± 0.15	12	0.44	(4)	-8.4	± 0.40	4	0.29	(3)	-8.2	± 0.18	6	0.71	(3)	-7.5	± 0.11	32	1.1	(3)
V:01	5.35	K195A	-7.7	± 0.17	20	0.70	(5)	-8.2	± 0.25	7	0.48	(3)	-9.7	± 0.20	0.22	0.02	(2)	-7.5	± 0.05	30	1.0	(4)
V:12	5.46	G206A	-7.3	± 0.21	47	1.6	(3)	-7.9	± 0.04	12	0.83	(3)	-8.8	± 0.10	2	0.19	(2)	-7.2	± 0.5	62	2.1	(3)
V:12	5.46	G206W	NA				(3)	NA				(3)	NA				(3)	NA				(3)
VI:13	6.48	W251A	-7.7	± 0.38	20	0.70	(3)	-8.3	± 0.14	4.7	0.32	(2)	-7.4	± 0.25	42	4.7	(4)	-7.5	± 0.41	29	0.97	(3)
VI:13	6.48	W251Q	-7.7	± 0.41	22	0.77	(3)	-7.8	± 0.14	15	1.0	(2)	-8.0	± 0.39	10	1.1	(3)	-7.5	± 0.41	29	0.97	(3)
VI:16	6.51	F254A	-6.6	± 0.19	278	9.7	(4)	-7.1	± 0.04	80	5.5	(3)	-8.0	± 0.12	10	1.2	(3)	-7.4	± 0.13	42	1.4	(3)
VI:20	6.55	L258A	-6.5	± 0.29	329	12	(3)	-7.5	± 0.08	35	2.4	(3)	-7.2	± 0.05	65	7.2	(5)	-7.2	± 0.08	64	2.1	(3)
VI:24	6.59	S262A	-7.2	± 0.13	61	2.1	(3)	-7.9	± 0.10	13	0.86	(3)	-8.1	± 0.28	8.9	1.0	(5)	-7.4	± 0.02	39	1.3	(3)
VII:02	7.35	T282A	-7.1	± 0.07	77	2.7	(3)	-7.5	± 0.10	31	2.1	(3)	-7.4	± 0.08	40	4.4	(3)	-7.0	± 0.06	93	3.1	(3)
VII:03	7.36	H283A	-7.5	± 0.08	30	1.0	(3)	-7.5	± 0.06	34	2.4	(3)	-7.8	± 0.11	17	1.9	(3)	-7.3	± 0.09	46	1.5	(3)
VII:06	7.39	E286A	<-5		>10000	>323	(3)	<-5		>10000	>689	(3)	<-5		>10000	>1100	(5)	<-5		>10000	>323	(3)
VII:09	7.42	S289A	-6.7	± 0.27	211	7.4	(3)	-7.5	± 0.04	34	2.3	(3)	-7.8	± 0.08	17	1.9	(3)	-7.4	± 0.02	36	1.2	(3)
VII:10	7.43	F290A	-7.4	± 0.24	41	1.4	(3)	-7.6	± 0.31	26	1.8	(3)	-7.7	± 0.34	21	2.3	(4)	-7.5	± 0.46	29	1.0	(3)

Figure 1

Human CCR8



LMD-009



ZK 756326

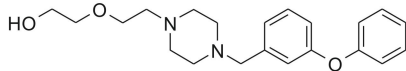


Figure 2

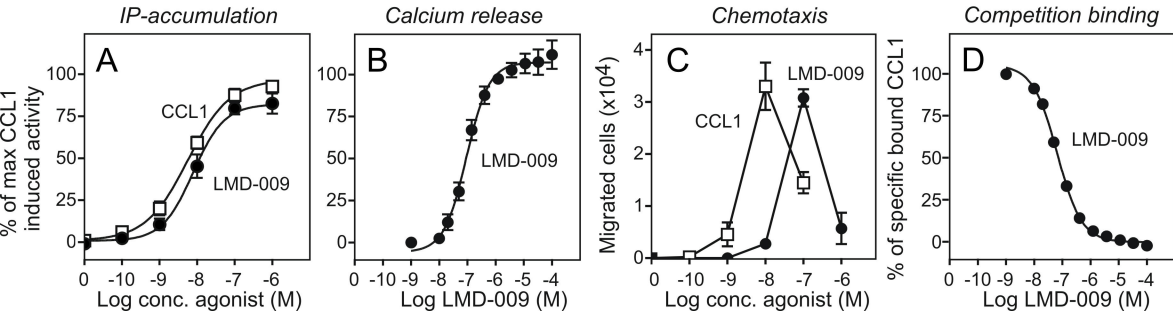


Figure 3

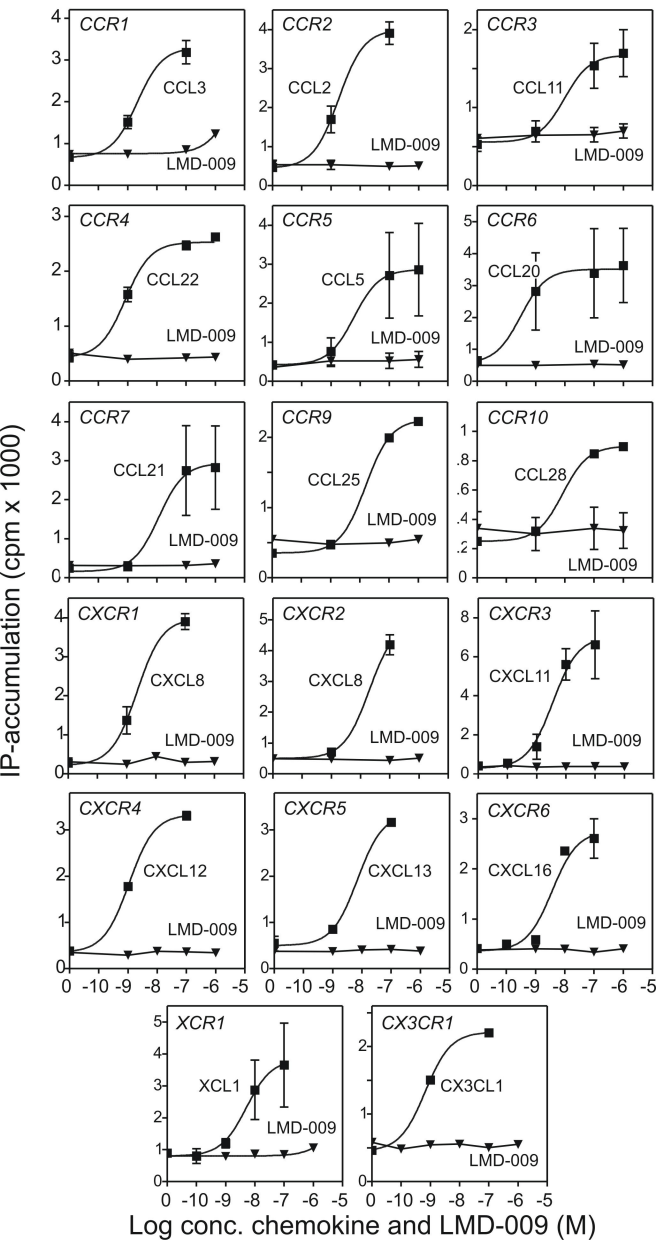


Figure 4

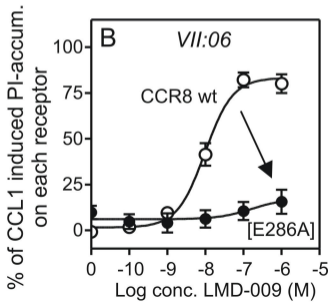
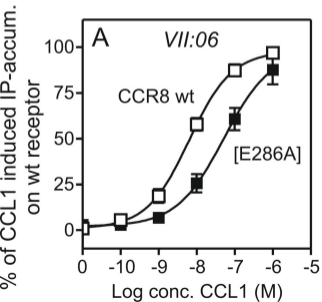


Figure 5

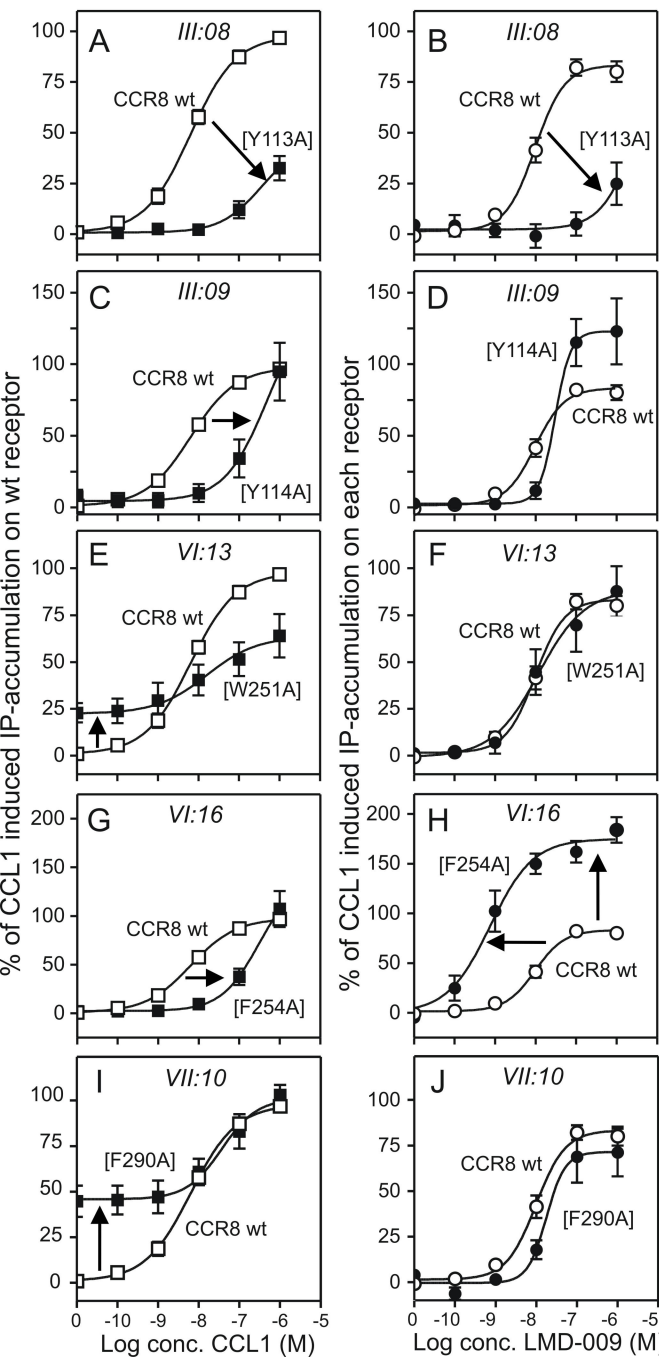
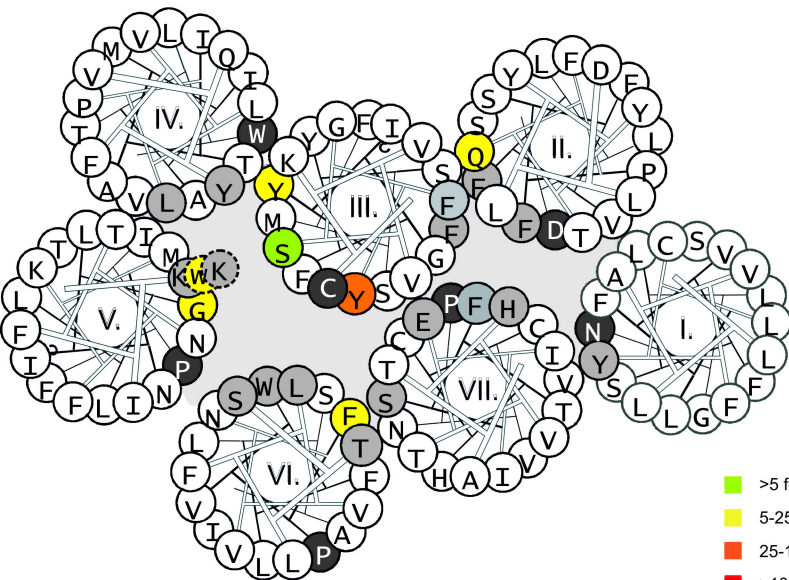


Figure 6

CCL1 (I-309)



LMD-009

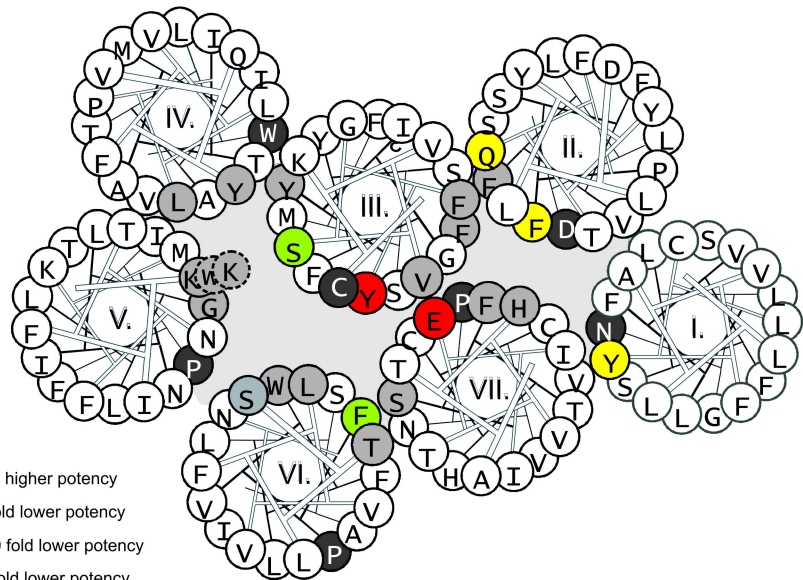


Figure 7

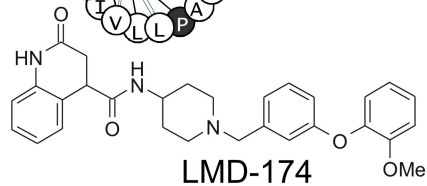
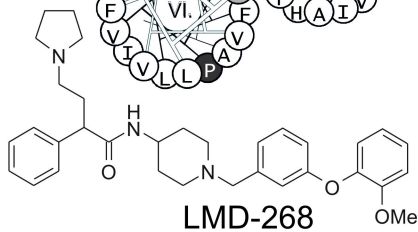
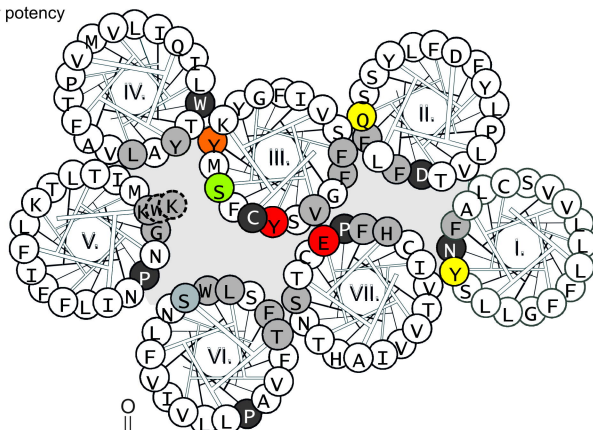
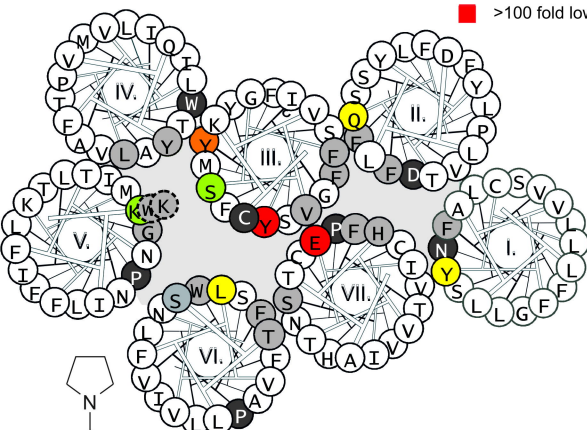
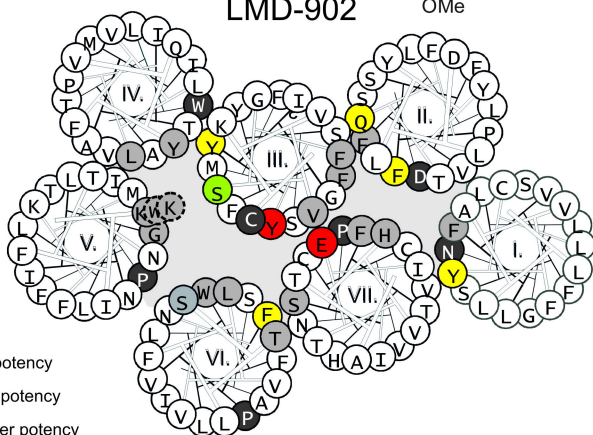
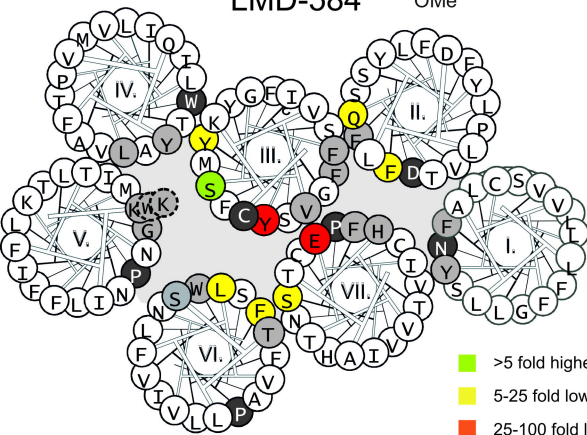
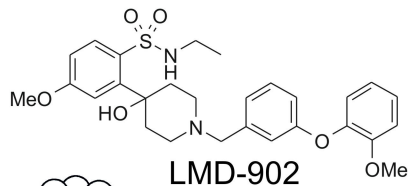


Figure 8

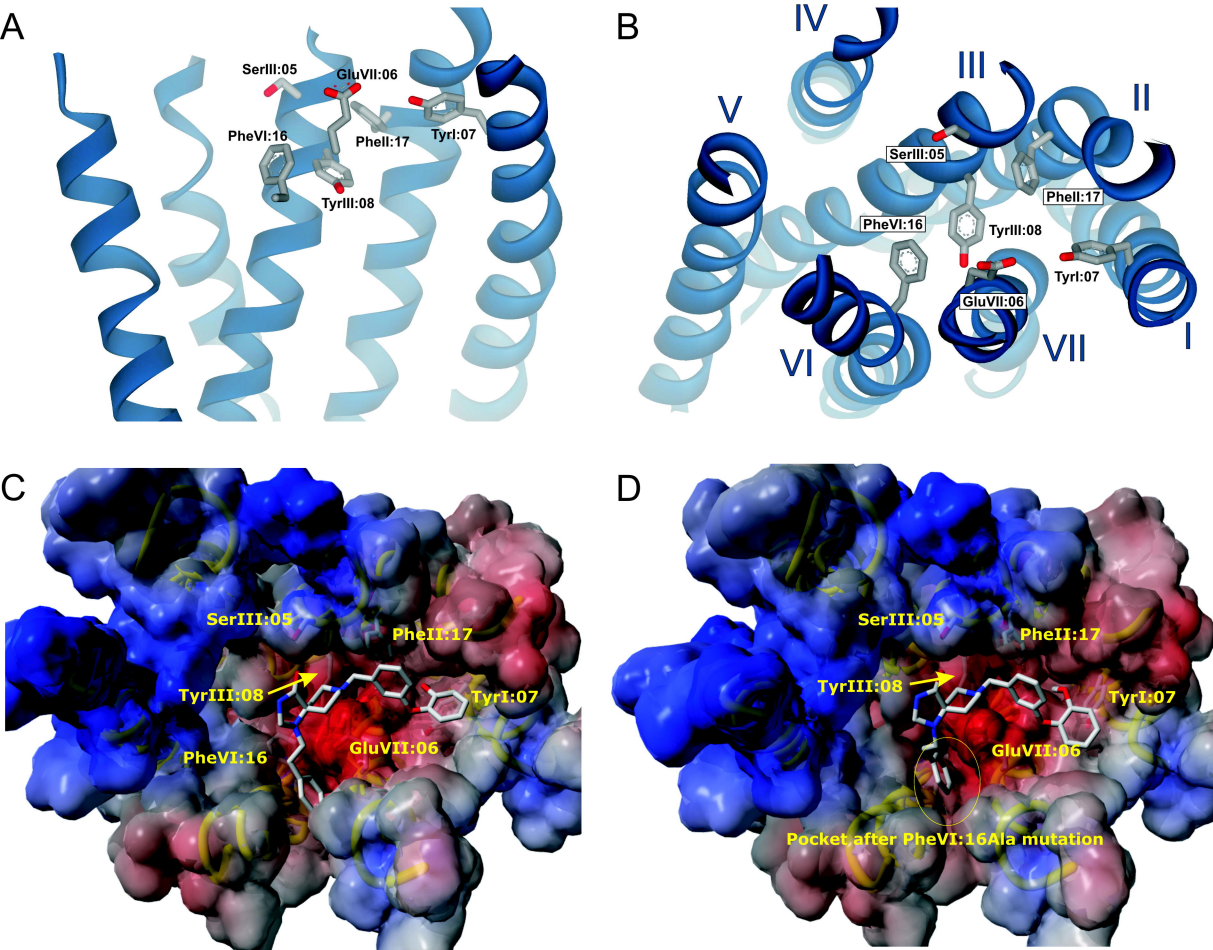


Figure 9

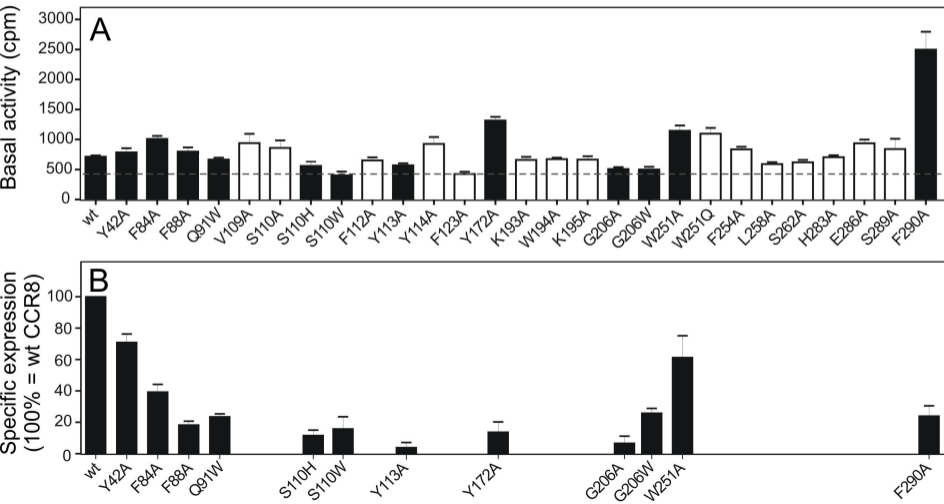


Figure 10

